Fiber-Grating-Based Self-Matched Additive-Pulse Mode-Locked Fiber Lasers

Ding-Wei Huang, Gang-Chih Lin, and C. C. Yang

***Abstract*— Fiber-grating-based self-matched additive-pulse mode-locked (APM) fiber lasers were investigated both theoretically and experimentally. With three fiber gratings to form the linearly coupled cavities, such a fiber laser system could generate stable mode-locked output without critical cavity length control. It was shown that the wavelength dependence of the effective penetration length of a fiber grating led to the self-matching of the cavity lengths of the coupled cavities. A millimeter-order cavity-length mismatch could be tolerated. In a similar laser structure using chirped fiber gratings with a designated arrangement of the grating polarities, the APM fiber laser could have the advantages of higher tolerance of cavity-length mismatch and stretched-pulse amplification. After pulse compression with a piece of single-mode fiber, output pulses with full-width at half-maximum pulsewidths of 930 fs were obtained.**

***Index Terms*—Delay effects, gratings, optical fiber lasers, optical pulse generation, pulsed lasers.**

I. Introduction

THE ADDITIVE-PULSE mode-locking (APM) technique was one of the key techniques for starting the era of ultrafast optics. It has been widely used for generating ultrashort pulses from various laser systems, including Nd:YAG, color-center, Ti:sapphire, and Er-doped fiber lasers. In this technique, the interference between two overlapping pulses from two coupled cavities, usually one containing the laser gain medium and the other containing a nonlinear medium for power-dependent phase modulation, could lead to pulse compression [1]. Because of the interfering nature of this mode-locking technique, typically a critical adjustment for matching the optical lengths of the two cavities was required [2]. In one implementation, a translation stage was generally needed for coarse adjustment and a piezoelectric transducer was required for fine adjustment. A servo-electronic circuit was used for mode-locking stabilization. For solid-state lasers with free-space external cavities, the configuration of linear coupled cavities was typically used for APM. However, this configuration is not suitable for all-fiber fiber lasers. This is so because, on the one hand, it is difficult to find a fiber component for dividing the two cavities; on the other hand, it is difficult to match the fiber lengths of the two cavities because of the nature of fiber splicing at the connections. Actually, the first pulsed fiber laser based on the concept of APM was implemented with one section of the coupled cavity in free space for cavity length matching [3]. However, such a laser configuration needs a complicated setup. Also, the ring-cavity polarization-APM configuration was used for all-fiber mode-locked fiber lasers [4]. Nevertheless, such a mode-locking process is based on nonlinear polarization evolution in the fiber which is different from the coupled-cavity mode-locking mechanism of concern in this paper.

Recently, APM fiber lasers with linearly coupled cavities formed with three fiber Bragg gratings were implemented [5], [6]. Without explanation, it was reported that critical cavity length control was unnecessary in achieving stable mode locking. The implementation of their APM fiber lasers implied the existence of a certain mechanism for self-matching the coupled cavities. According to our study, this simple mode-locking operation is attributed to the fact that a fiber grating can serve as a wavelength-dependent delay component. In other words, the effective penetration length into a fiber grating depends on the operating wavelength. Hence, the effective optical lengths including the parts penetrating into the fiber gratings of the two coupled cavities can be self-matched by self-adjustment of the oscillating wavelength. The detailed theory of this self-matching mechanism is the first part covered in this paper. The same mechanism works in coupled cavities formed with chirped fiber gratings. With chirp, the self-matching mechanism is more efficient. In other words, a larger cavity mismatch can be tolerated. Besides, with high group-delay dispersion (GDD) contributed from the chirped fiber gratings, the laser could have the advantage of stretched-pulse amplification [7]. Because of the anomalous group-velocity dispersion (GVD) nature of a typical single-mode fiber near 1550 nm, usually a mode-locked fiber laser results in the generation of soliton-like pulses [1]. However, because the formation of solitons sets a limit to the output pulse energy, nonsoliton output is preferred for achieving a higher output pulse energy [8]. This goal can be reached by making the effective GVD positive inside the laser cavity. With positive GVD, the output pulse width is stretched and the pulse can be amplified without the soliton limit. This mechanism is called stretched-pulse amplification. In such a design, a piece of fiber with negative GVD at the operating wavelength is usually needed after the laser output port for compressing the pulse. In our study, we found that with a designated arrangement of chirped grating polarities, the laser configuration led to not only to efficient self-matching of cavity lengths but also a positive effective GVD inside the main cavity for pulse stretching. The design, simulation, and experimental imple-

Manuscript received June 29, 1998; revised October 16, 1998. This work was supported by the National Science Council, R.O.C., under Grant NSC 87-2215-E-002-006, Grant NSC 87-2215-E-002-007, Grant NSC 86-2212-M-002-024, Grant NSC 86-2215-E-002-010, and Grant NSC 86-2215-E-002-011.

The authors are with the Department of Electrical Engineering and the Institute of Electro-Optical Engineering, National Taiwan University, Taipei, Taiwan, R.O.C.

Publisher Item Identifier S 0018-9197(99)00862-3.

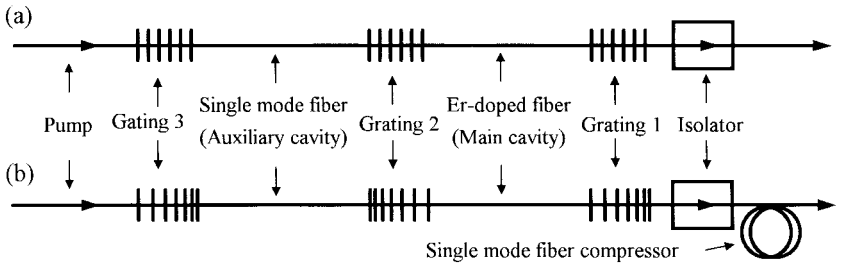

Fig. 1. System configuration of a linear coupled-cavity APM fiber laser formed with (a) uniform fiber gratings and (b) chirped fiber gratings.

mentation of such a mode-locked fiber laser are also covered in this paper. In Section II, theoretical analysis is presented and the results of numerical simulations are given in Section III. Then, the experimental procedures and results are discussed in Section IV. Finally, conclusions are drawn in Section V.

II. Theoretical Analysis

The system configuration is shown in Fig. 1 for coupled cavities formed with (a) uniform fiber gratings and (b) chirped fiber gratings. Between the three fiber gratings, the main cavity contains a piece of Er-doped fiber and the auxiliary cavity contains a piece of communication single-mode fiber.

A. Cavity Length Self-Matching

The basic idea for cavity length self-matching is that a fiber grating serves as a wavelength-dependent delay line. For a given cavity length mismatch within a certain range, the laser system can find a suitable oscillating wavelength at which the difference of the group delay between the gratings used can compensate for the cavity length mismatch. The tolerance range for cavity mismatch depends on various parameters, including grating length, grating reflectivity, chirp of the grating and the differences between the gratings. To understand this phenomenon quantitatively, we start with the reflection coefficient $r(\omega)$ and transmission coefficient $t(\omega)$ of a uniform fiber grating which are expressed as [9]

$$r(\omega) = \frac{-j\kappa \sinh(L\sqrt{\kappa^2-\delta^2})}{\sqrt{\kappa^2-\delta^2}\cosh(L\sqrt{\kappa^2-\delta^2}) + j\delta\sinh(L\sqrt{\kappa^2-\delta^2})} \tag{1}$$

$$t(\omega) = \frac{\sqrt{\kappa^2-\delta^2}}{\sqrt{\kappa^2-\delta^2}\cosh(L\sqrt{\kappa^2-\delta^2}) + j\delta\sinh(L\sqrt{\kappa^2-\delta^2})} \tag{2}$$

where L is the grating length, κ is the coupling coefficient in the grating, and δ is defined as $\delta = \beta(\omega) - \beta_o \approx \beta_o'(\omega - \omega_o) = (\omega - \omega_o) = (\omega - \omega_o)/v_g$, where $\beta(\omega)$ is the propagation constant in the fiber, β_o is that at the signal central frequency ω_o, and v_g is the group velocity. If we designate the higher refractive-index as n_1 and the average refractive-index of the fiber as n_0 ($n_1 > n_0$), then κ is given by $\kappa = \omega(n_1^2 - n_0^2)/2n_0c$, where c is the speed of light in vacuum. The group delay time of the reflected signal $T_r(\omega)$ is the derivative of the phase shift $\phi_r(\omega)$ as

$$T_r(\omega) = -\frac{d}{d\omega}\phi_r(\omega) = -\frac{d}{d\omega}\arg(r(\omega)). \tag{3}$$

It is noted that $r(\omega)$ is typically complex. Now, we define an effective penetration length into a grating corresponding to the delay distance of the grating as

$$\Delta L(\omega) = \frac{v_g T_r(\omega)}{2} \tag{4}$$

where the factor of two in the denominator accounts for the round trip of the reflected signal in the grating.

To show the basic idea of cavity self-matching, we first consider the case of the APM laser structure with coupled cavities using uniform fiber gratings. From (4), we can derive an analytical form of the effective penetration length for a uniform fiber grating as

$$\Delta L(\omega) = \frac{\kappa^2\cosh(L\sqrt{\kappa^2-\delta^2})\sinh(L\sqrt{\kappa^2-\delta^2}) - L\delta^2\sqrt{\kappa^2-\delta^2}}{2\sqrt{\kappa^2-\delta^2}[\kappa^2\cosh^2(L\sqrt{\kappa^2-\delta^2}) - \delta^2]}. \tag{5}$$

Fig. 2 shows the reflectance and the effective penetration length of a uniform fiber grating with $L = 6$ mm and $\kappa = 730\ \text{m}^{-1}$. The effective penetration length of a uniform fiber grating is symmetric in frequency and between the two input directions. In other words, the effective penetration length is the same for signals reflected from both sides of a uniform fiber grating. Different grating lengths lead to quite different effective penetration lengths. Note that for a uniform grating the effective penetration lengths near the edges of the reflection window can be longer than the grating length. This is due to the reduced group velocities at those wavelengths. In our laser system, because the central grating (grating 2) in Fig. 1(a) causes equal delay time for the two cavities, it actually makes no contribution to cavity length matching. The cavity length mismatch is compensated by the difference of the effective penetration length between gratings 1 and 3, i. e.,

$$\Delta L_3(\omega) - \Delta L_1(\omega) = L_M - L_A \tag{6}$$

where L_M and L_A represent the physical lengths of the main cavity and the auxiliary cavity, respectively. Meanwhile, $\Delta L_1(\omega)$ and $\Delta L_3(\omega)$ stand for the effective penetration lengths of the uniform fiber gratings 1 and 3, respectively. For a given mismatch within the tolerance range, the laser system can find an oscillating wavelength so that (6) is satisfied. Under the condition that the cavity length mismatch is compensated, the additive-pulse mode-locking interaction can be expected for generating short pulses.

Because of the ripples in the group delay response of a chirped fiber grating with uniform index variation, it is not

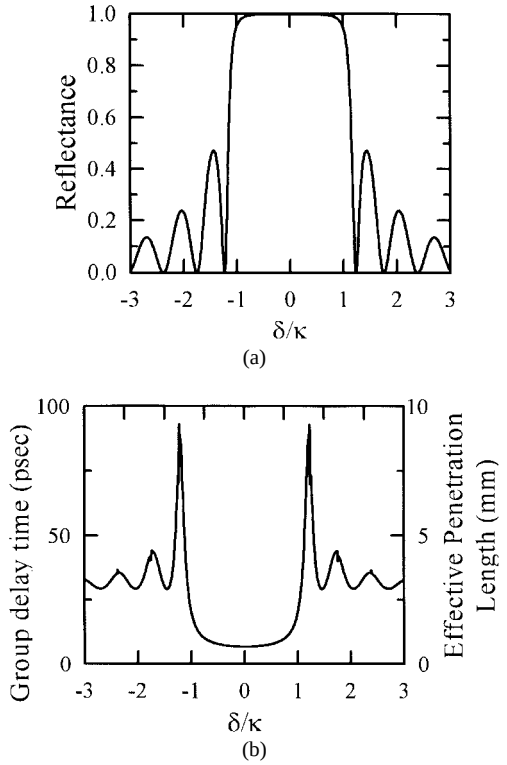

Fig. 2. (a) Reflectance and (b) effective penetration length of a uniform fiber grating.

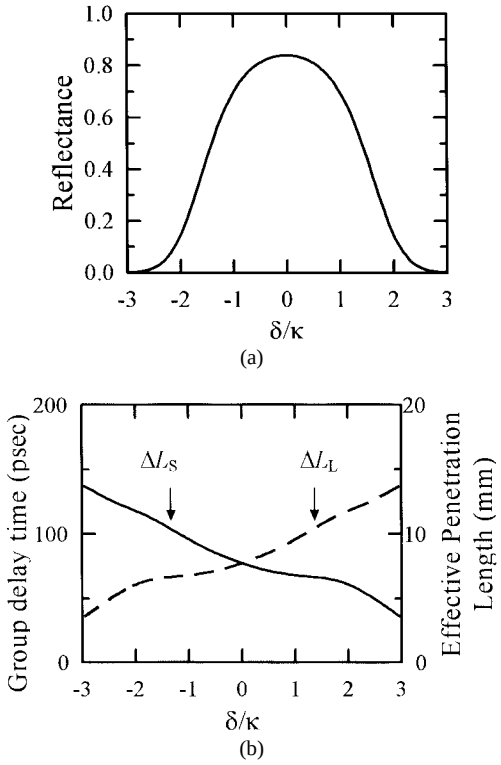

Fig. 3. (a) Reflectance and (b) effective penetration lengths $(\Delta L_{L(S)})$ of a chirped fiber grating (from the large (small)-period side).

suitable for applications, particularly those in connection with dispersion compensation [10] and cavity length matching. This problem can be overcome by using chirped fiber gratings with apodization. Fig. 3 shows the reflectivity and effective penetration length of an apodized chirped fiber grating with $L = 16$ mm, $\kappa = 360\ \mathrm{m}^{-1}$, and a Gaussian-apodized refractive-index profile. Here, we can clearly see quite different characteristics of an apodized chirped fiber grating from a uniform one. Since we will be always concerned with chirped gratings with apodization, the word "apodized" is neglected in the following. The effective penetration length of a chirped fiber grating is asymmetric in frequency and between the two input directions. In fact, the effective penetration lengths for signals reflected from the large-period side and the small-period side of a chirped fiber grating are nearly complementary. Intuitively, the effective penetration length of a chirped fiber grating is the length between the grating input end and the position where the corresponding Bragg wavelength of the grating period equals the signal wavelength. Hence, complementary effective penetration lengths from the two sides are expected. For cavity length self-matching, chirped gratings are actually more effective than uniform gratings because, in a chirped grating, the curve of the effective penetration length is nearly linear and the slope is larger. This means that with the same wavelength shift a larger cavity length mismatch can be compensated. In a coupled-cavity configuration with chirped gratings, contrary to the uniform grating case, the central chirped grating (grating 2) causes different delay times for the two cavities and hence makes a significant contribution to cavity length matching. Also, the polarities (from the large-period or small-period side) of the three chirped gratings would affect the effective cavity lengths of the two coupled cavities. To compensate for the cavity length mismatch, the differences of the effective penetration lengths among three gratings including their polarities must be taken into account. For the case depicted in Fig. 1(b), this relation can be formulated as

$$\Delta L_{1L}(\omega)+\Delta L_{2L}(\omega)-\Delta L_{2S}(\omega)-\Delta L_{3S}(\omega) = L_A - L_M \tag{7}$$

where $\Delta L_1(\omega), \Delta L_2(\omega)$, and $\Delta L_3(\omega)$ denote the effective penetration lengths of the three chirped gratings, and the subscripts L and S represent the situations in which the signal is reflected from the large- and small-period sides, respectively.

B. Stretched-Pulse APM Using Chirped Fiber Gratings

The GDD of a fiber grating plays an important role in the effective GVD of a laser cavity. The GDD of a fiber grating is the derivative of the group delay as

$$D_r(\omega) = \frac{d}{d\omega} T_r(\omega). \tag{8}$$

Chirped gratings with different grating polarities have different signs of GDD values. For a chirped grating, the GDD is positive from the large-period side and negative from the small-period side. Usually, the GDD value of a uniform grating is relatively small. Hence, the effective GVD of a laser cavity is not significantly affected by the uniform gratings. However, the GDD value of a chirped grating can be quite larger, compared with the intrinsic GVD value of a piece of single-mode fiber of several meters in length. Hence, the effective intracavity GVD is dominated by the chirped gratings. To

stretch the pulse for the purpose of increasing the pulse energy, we can arrange the three chirped gratings in a way that the large-period sides face the main cavity and the small-period sides face the auxiliary cavity. This leads to the result that the oscillating pulses experience highly positive effective GVD in the main cavity and highly negative effective GVD in the auxiliary cavity. For calculation simplicity, the frequency dependence of the reflection coefficient of a chirped grating is assumed to follow a parabolic function such as

$$r_{L(S)}(\omega) \cong r_o\left(1-\frac{(\omega-\omega_o)^2}{\Omega_o^2}\right)\exp[j(\phi_{L(S)} + T_{L(S)}(\omega-\omega_o)+D_{L(S)}(\omega-\omega_o)^2)] \quad (9)$$

where r_o is the reflection coefficient at the central wavelength, Ω_o is the bandwidth of the reflection window, and ϕ, T, and D are the phase shift, group delay time, and GDD at the central oscillating frequency ω_o, respectively. Meanwhile, the subscripts L and S denote the polarities of the chirped gratings as defined in (7). With this approximation, we build an equation system [see (10)] based on the nonlinear Schrödinger equation including the effects of: 1) gain constant g; 2) gain bandwidth Ω_g; 3) GVD factors D_M, D_A, and D_C; and 4) self-phase modulation of the fibers in the main cavity, auxiliary cavityc and output compressor (the fiber used to compress the pulses after the laser output port), respectively. The equation system also contains the parameters of the three chirped gratings including the reflection coefficients r_1, r_2, r_3, the bandwidths of the reflection windows $\Omega_1, \Omega_2, \Omega_3$, and the GDD D_{1L}, D_{2L}, D_{2S}, and D_{3S} with the designated grating polarities. The equations for various scalar wave fields $a_1, a_2, b_1, b_2, b_1', b_2', c$, and c', as defined in Fig. 4 (except for the output wave field c', all the wave fields are defined at the connecting points of cavity fibers and gratings), are given as

$$b_1 = r_2\left(1+\frac{1}{\Omega_2^2}\frac{d^2}{dt^2}+jD_{2L}\frac{d^2}{dt^2}\right)a_1 + a_2\sqrt{1-r_2^2} \quad (10a)$$

$$b_2 = r_2\left(1+\frac{1}{\Omega_2^2}\frac{d^2}{dt^2}+jD_{2S}\frac{d^2}{dt^2}\right)a_2 - a_1\sqrt{1-r_2^2} \quad (10b)$$

$$b_1' = \left[1+g\left(1+\frac{1}{\Omega_g^2}\frac{d^2}{dt^2}\right) + jD_M\frac{d^2}{dt^2} - j\delta_M|b_1|^2\right]b_1 \quad (10c)$$

$$b_2' = \left[1+jD_a\frac{d^2}{dt^2} - j\delta_a|b_2|^2\right]b_2 \quad (10d)$$

$$a_1 = \left[1+g\left(1+\frac{1}{\Omega_g^2}\frac{d^2}{dt^2}\right)+\frac{1}{\Omega_1^2}\frac{d^2}{dt^2} + j(D_M+D_{1L})\frac{d^2}{dt^2} - j\delta_M|b_1'|^2\right]r_1 b_1' \quad (10e)$$

$$a_2 = \left[1+\frac{1}{\Omega_3^2}\frac{d^2}{dt^2}+j(D_A+D_{3S})\frac{d^2}{dt^2} - j\delta_a|b_2'|^2\right]r_3 b_2' \quad (10f)$$

$$c = -b_1'\sqrt{1-r_1^2} \quad (10g)$$

and

$$c' = \left(1+jD_C\frac{d^2}{dt^2} - j\delta_C|c|^2\right)c. \quad (10h)$$

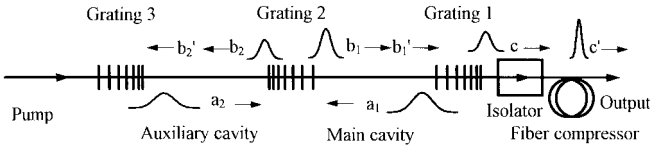

Fig. 4. Detailed setup of the fiber laser with linearly coupled cavities formed with chirped fiber gratings.

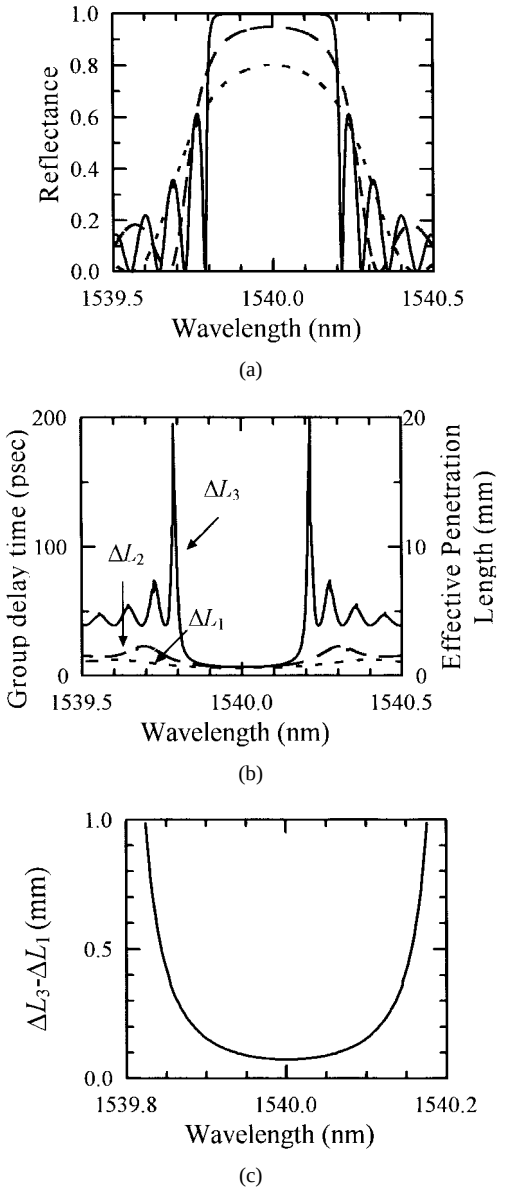

Fig. 5. (a) Reflectance and (b) effective penetration lengths of the three uniform gratings used in Fig. 1(a). (c) $\Delta L_3 - \Delta L_1$ as a function of the oscillating wavelength.

In the equations above, self-phase modulation effects are denoted by $\delta_{M(A,C)} = n_2\omega_o L_{M(A,C)}/c$, where L_C represents the physical length of the fiber compressor. Equations (10a)–(10h) were derived based on the master equation in [1] with the following factors taken into account: 1) the bandwidths of the reflection windows of the gratings as defined in (9) and 2) the signs and magnitudes of the group delay dispersion of the three chirped gratings. Meanwhile,

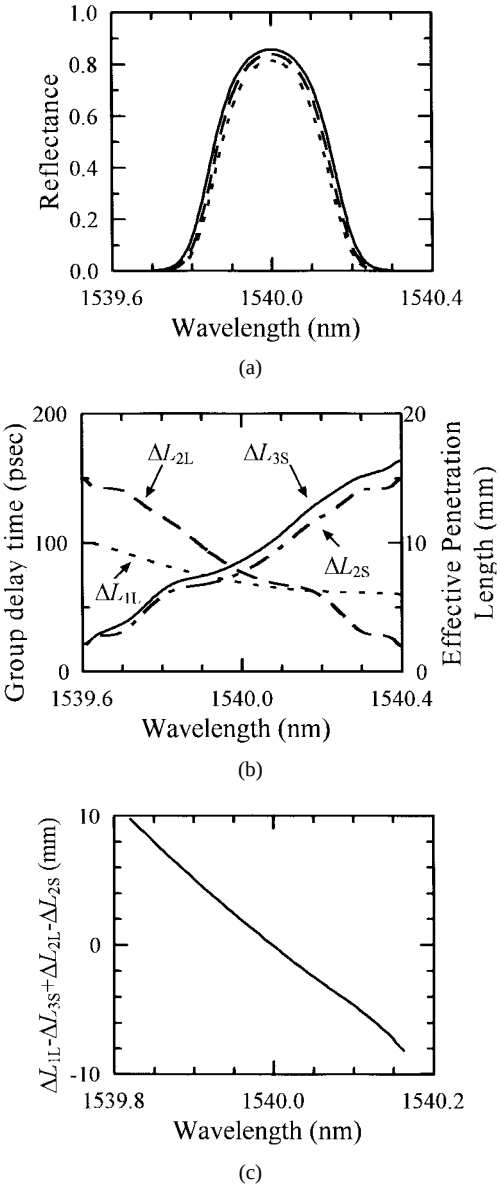

Fig. 6. (a) Reflectance and (b) effective penetration lengths of the three chirped gratings used in Fig. 1(b). (c) $\Delta L_{1L} - \Delta L_{3S} + \Delta L_{2L} - \Delta L_{2S}$ as a function of the oscillating wavelength.

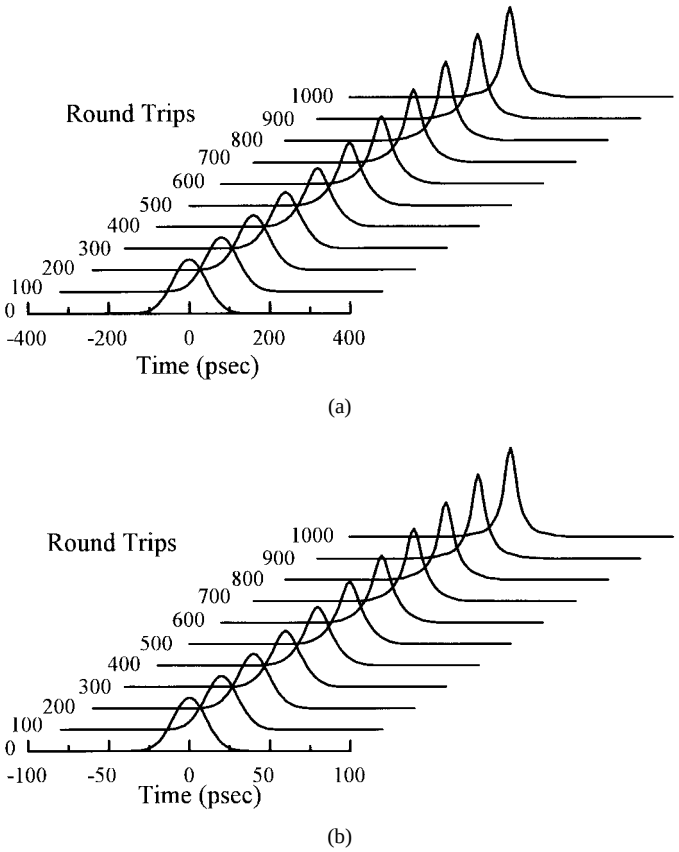

Fig. 7. Simulation results of pulse evolution just from the output gratings in Fig. 1(a) and (b), respectively, under the condition that the oscillating wavelength is self-adjusted so that the cavity length mismatch is compensated for.

the following two assumptions were made to simplify the derivations.

1) The reflectivities and reflection window bandwidths of gratings 1 and 3 are sufficiently large so that they can be regarded as two high-reflection mirrors.
2) The group delay response in transmitting a grating is assumed to be independent of wavelength since it is almost a constant.

Equations (10a)–(10h) were numerically solved to simulate pulse evolution in such a coupled-cavity laser.

Before presenting our numerical results, let us first give the procedure for solving those equations. This procedure provides a qualitative description of the evolution of the signals in the coupled cavities. We start with a transient signal or long pulse which may come from noise. At the beginning, the laser system picks up the oscillating wavelength at which the coupled cavities are matched [described by (7)]. After that, the pulsed signal begins to have additive-pulse interactions [described by (10a)–(10f)]. The pulse in the main cavity is stretched with highly positive dispersion while reflected from the large-period side of the chirped gratings. The stretched pulse receives more gain without significant gain saturation. Meanwhile, the pulse in the auxiliary cavity is stretched with highly negative dispersion while reflected from the small-period side of the chirped gratings. Hence, the pulses in the two cavities have opposite signs of chirp. When the pulses from the two cavities combine near the central grating, the two pulses have coherent additive-pulse interactions only near their peaks. As a result, the pulse in the main cavity is shortened after each round trip. When the stretching and shortening effects reach balance, stable pulses with positive chirping can be obtained from the output grating. After passing through the output grating [described by (10g)], the positively chirped output pulse is shortened through self-phase modulation and dispersion compensation in the output fiber compressor [described by (10h)].

III. Numerical Simulations

In the simulations, the parameter values used for the coupled cavities included: the GVD of the fiber at $\beta_o'' = 0.04$ ps^2/m, the nonlinear refractive-index at $n_2 = 3 \cdot 2 \cdot 10^{-16}$ cm^2/W, and the gain constant in the main cavity at $g = 3 \cdot 10^{-4}$ cm^{-1}.

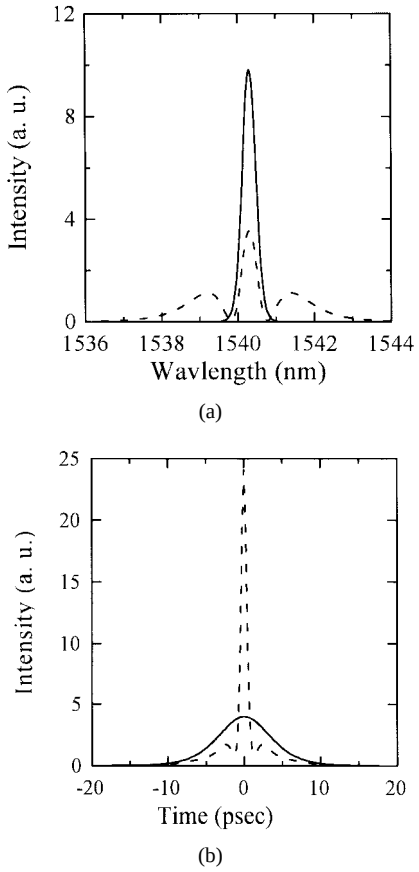

Fig. 8. Simulation results of (a) the spectra and (b) the pulse shapes of the uncompressed (solid curves) and compressed pulses (dashed curves).

The effective refractive index was 1.46 of the fiber and the index change in the gratings was $1.78{\cdot}10^{-4}$. The lengths of the uniform gratings used in Fig. 1(a) were 2, 3, and 8 mm for gratings 1, 2, and 3, respectively. The parameter values for chirped gratings included: the grating chirp at 0.2 nm/cm and the grating lengths at 16, 17, and 18 mm for gratings 1, 2, and 3 in Fig. 1(b), respectively. All the fiber gratings were assumed to have the same center Bragg wavelength at 1540 nm. The lengths of the two coupled cavities were near 2.3 m with cavity length mismatches of 0.14 mm in Fig. 1(a) and 2 mm in Fig. 1(b). The peak power and pulsewidth of the initial Gaussian pulse were set at 6 mW and 1 ns, respectively.

Fig. 5(a) and (b) show the reflectance, group delay times, and effective penetration lengths, respectively, of the three uniform gratings used in Fig. 1(a). Fig. 5(c) shows the value $\Delta L_3 - \Delta L_1$ as a function of the oscillating wavelength. Fig. 6(a) and (b) shows the corresponding values of the three chirped gratings used in Fig. 1(b). Meanwhile, Fig. 6(c) shows the value $\Delta L_{1L} - \Delta L_{3S} + \Delta L_{2L} - \Delta L_{2S}$ as a function of the oscillating wavelength. Figs. 5(c) and 6(c) provide the information about the wavelength adjustment for compensating a certain cavity length mismatch. The maximum compensating capability is limited by the reflection windows of the used gratings. Fig. 7(a) and (b) demonstrate the evolution of the output pulses right from the output gratings as in Fig. 1(a) and (b), respectively, under the condition that the oscillating wavelength has been self-adjusted to compensate for the cavity

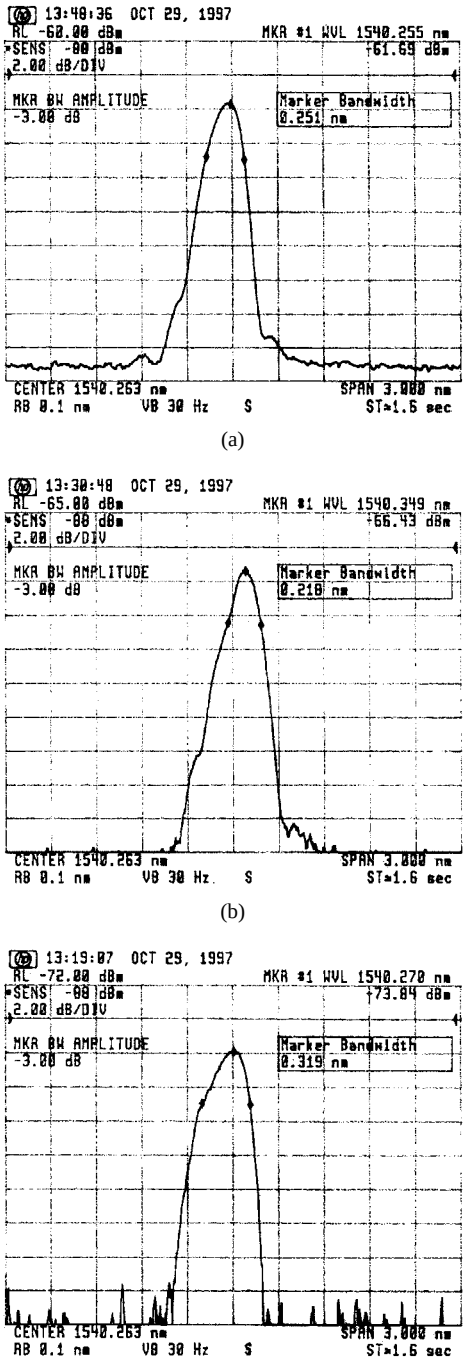

Fig. 9. Measured reflectance spectra of the three chirped fiber gratings used in Fig. 1(b). (a) Grating 1, (b) grating 2, and (c) grating 3.

length mismatch. We can see that in either case the pulse is first compressed and eventually reaches a steady state. This implies the feasibility of mode locking. In Fig. 7(a), the oscillating wavelength is self-adjusted to 1540.1016 nm, at which the cavity length mismatch (assumed to be 0.14 mm) is just the same as the value of $\Delta L_3 - \Delta L_1$. It was shown that at oscillating wavelengths other than this value, the pulse became broadened and vanished after a certain number of round trips. In Fig. 7(b), the oscillating wavelength is self-adjusted to 1540.04 nm, at which the cavity length mismatch (assumed to be 2 mm) is just the same as the

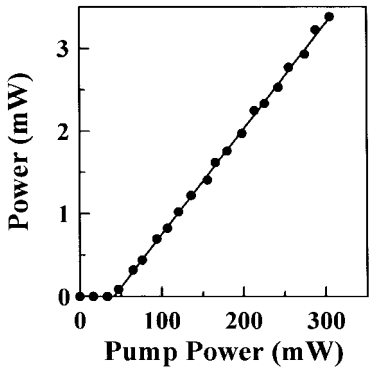

Fig. 10. Output power as a function of the pump power from the fiber laser formed with chirped gratings.

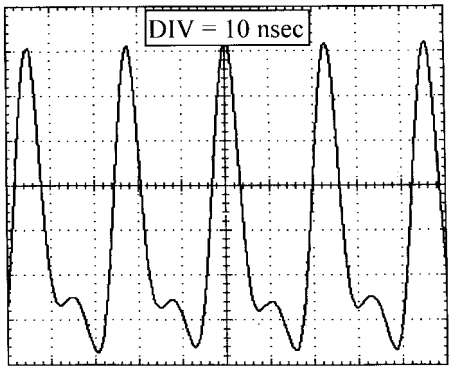

Fig. 11. Output pulse train of the fiber laser formed with chirped gratings.

value $\Delta L_{1L} - \Delta L_{3S} + \Delta L_{2L} - \Delta L_{2S}$. It was also shown that at an oscillating wavelength other than this value, a steady pulse could not be obtained. Note that the output pulses in Fig. 7(b) are those right after the output grating and should be positively chirped. After pulse compression, the pulsewidth becomes smaller. Fig. 8(a) and (b) shows the spectra and pulse shapes of the uncompressed (solid curves) and compressed (dashed curves) pulses. The spectrum of the pulse becomes broadened due to self-phase modulation in the fiber compressor. Meanwhile, the pulsewidth is shortened due to anomalous GVD in this fiber.

IV. Experimental Procedures and Results

In our experiments, the fabricated fiber laser has the configuration shown in Fig. 1(b). We used a highly Er-doped fiber (2700 ppm) of 1.9 m in length in the main cavity. The parameter values of the used fiber gratings and fiber are the same as those described in Section III for the simulations. The chirped fiber gratings were fabricated with a chirped phase mask by exposing to UV laser pulses at 248 nm. During the fabrication process, the UV laser beam was in a nearly Gaussian profile. Hence, the chirped fiber gratings were expected to be apodized. Fig. 9 shows the measured reflectance spectra of the three chirped fiber gratings. All the fiber elements were spliced together and the cavity lengths were controlled to within an accuracy of 1 mm. Note that it was almost impossible to match the cavity length within wavelength-order accuracy while splicing the fiber elements.

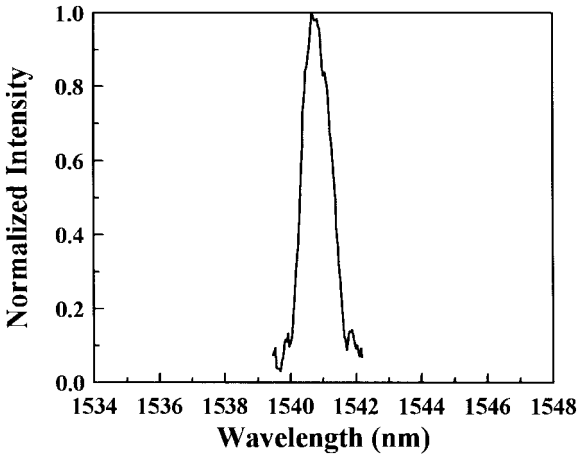

(a)

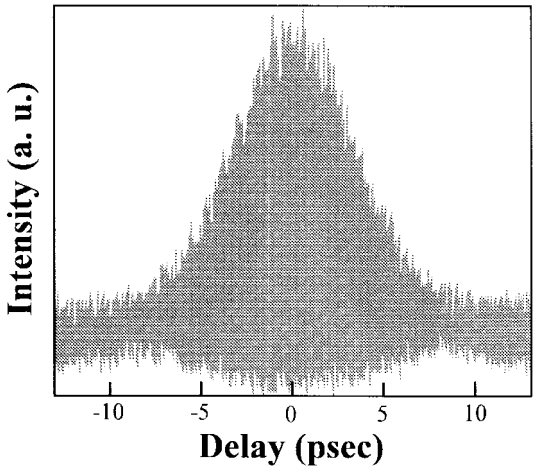

(b)

Fig. 12. Experimental results of (a) spectrum and (b) autocorrelation trace of the output pulse right after the isolator.

A CW Ti:sapphire laser at 980 nm was used for pumping the fiber laser. Fig. 10 shows the output power as a function of the pump power. The lasing threshold was 40 mW and the slope efficiency was about 1.2%. When the pump power was above 90 mW, stable pulse trains could be observed (see Fig. 11). The 43.9-MHz pulse repetition rate is consistent with the cavity length of 2.34 m. To confirm the effect of stretched-pulse amplification, we observed the pulse evolution along the fiber compressor. Fig. 12(a) and (b) show the spectrum and autocorrelation trace, respectively, of the output pulse right after the isolator (about 2.5-m fiber length from the output grating). The pulse here had a spectral width of 0.7 nm and a full-width at half-maximum (FWHM) pulse of 5.5 ps. The time-bandwidth product was 0.487, which was 1.55 times larger than a transform-limited pulse. This is as expected because the output pulse should be positively chirped. Note that autocorrelation was measured with the technique of two-photon absorption in a light-emitting diode at 933 nm. Then, the fiber compressor was spliced to the output end of the isolator. It was observed that the pulsewidth became shorter and shorter along the fiber length. Due to self-phase modulation, the spectral width became broadened. At 12 m

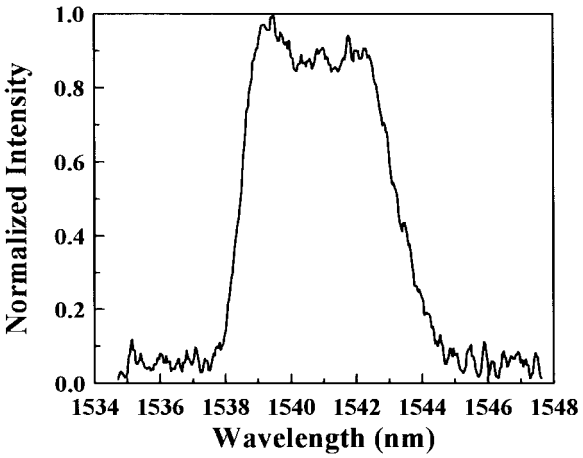

(a)

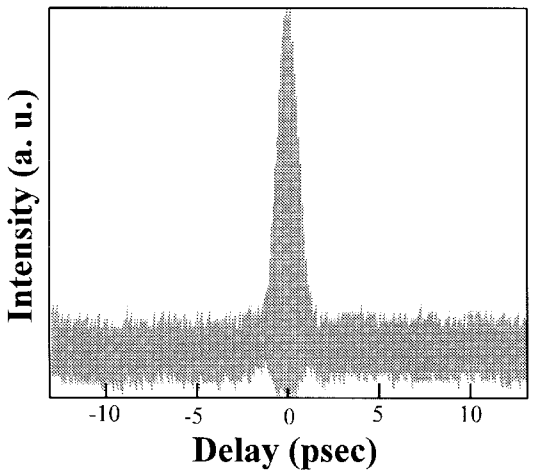

(b)

Fig. 13. Experimental results of (a) spectrum and (b) autocorrelation trace of the pulse at a fiber length of 12 m from the output grating.

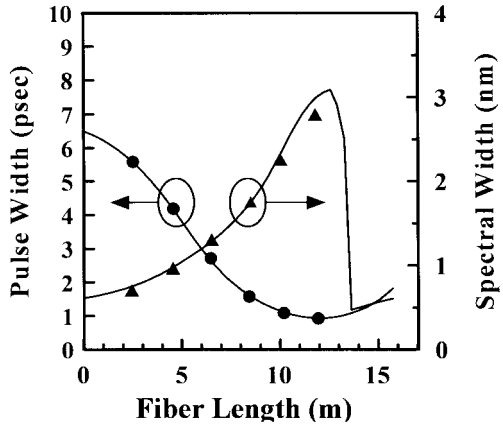

Fig. 14. Comparisons between the experimental and simulation results (solid curves) of the output spectral width (filled triangles) and pulsewidth (filled circles) at different lengths of the fiber compressor.

from the output grating, the shortest pulse width was obtained. Fig. 13(a) and (b) show the spectrum and autocorrelation trace, respectively, of the pulse at this point. The spectral width was 2.75 nm and the FWHM pulse duration was 930 fs, leading to a time-bandwidth product of 0.324. This implies that nearly transform-limited pulses were obtained. Fig. 14 shows the measured evolution of the pulsewidth (filled circles) and the spectral width (filled triangles) of the pulse along the fiber compressor. The solid curves represent the simulation results obtained by numerically solving (10a)–(10h). Good agreement between the experimental and simulation results can be clearly seen in Fig. 14.

V. Conclusions

We have theoretically and experimentally investigated the self-matching mechanism of the APM fiber lasers with linearly coupled cavities formed with fiber gratings. A stretched-pulse APM mode-locked fiber laser using chirped fiber gratings was proposed and successfully implemented. The cavity length mismatch of the coupled cavities could be automatically compensated by self-adjusting the oscillating wavelength. The wavelength-order cavity length control in the conventional APM technique became unnecessary. Using apodized chirped fiber gratings, the APM fiber laser could have the advantages of cavity length self-matching and stretched-pulse amplification. With an appropriate compression process, almost transform-limited pulses with a FWHM pulse of 930 fs were obtained. The pulsewidth of such a mode-locked fiber laser was limited by the reflection windows of the chirped gratings that were used. Currently, we are fabricating gratings with an even higher chirp for achieving a wider grating reflection window so that a shorter pulse can be obtained.

Acknowledgment

The assistance of C.-C. Yang in the Industrial Technology Research Institute, Hsin Chu, Taiwan, in fabricating fiber gratings is appreciated.

References

[1] H. A. Haus, J. G. Fujimoto, and E. P. Ippen, "Structures for additive pulse mode locking," *J. Opt. Soc. Amer. B*, vol. 8, pp. 2068–2076, Oct. 1991.
[2] F. M. Mischke and L. F. Mollenauer, "Stabilizing the soliton laser," *IEEE J. Quantum Electron.*, vol. QE-22, pp. 2242–2250, 1986.
[3] L. F. Mollenauer and R. H. Stolen, "The soliton laser," *Opt. Lett.*, vol. 9, pp. 13–15, 1984.
[4] H. A. Haus, E. P. Ippen, and K. Tamura, "Additive pulse mode locking in fiber lasers," *IEEE J. Quantum Electron.*, vol. 30, pp. 200–208, Jan. 1994.
[5] P. K. Cheo, V. G. Mutalik, and, G. A. Ball, "Mode-locking of in-line coupled-cavity fiber lasers using intra-core Bragg gratings," *IEEE. Photon. Technol. Lett.*, vol. 7, pp. 980–982, Sept. 1995.
[6] P. K. Cheo, L. Wang, and, M. Ding, "Low-threshold, self-tuned and passively mode-locked coupled-cavity all-fiber lasers," *IEEE Photon. Technol. Lett.*, vol. 8, pp. 66–68, Jan. 1996.
[7] H. A. Haus, K. Tamura, L. E. Nelson, and E. P. Ippen, "Stretched-pulse additive pulse mode-locking in fiber ring lasers: Theory and experiment," *IEEE J. Quantum Electron.*, vol. 31, pp. 591–598, Mar. 1995.
[8] K. Tamura and M. Nakazawa, "Optimizing power extraction in stretched-pulse fiber ring lasers," *Appl. Phys. Lett.*, vol. 67, pp. 3691–3693, Dec. 1995.
[9] T. Tamir, *Integrated Optics*, 2nd Ed. New York: Springer-Verlag, 1979.
[10] K. Ennser, M. N. Zervas, and R. I. Laming, "Optimization of apodized linearly chirped fiber gratings for optical communications," *IEEE J. Quantum Electron.*, vol. 34, pp. 770–778, May 1998.

Ding-Wei Huang was born in Hua Lian, Taiwan, in 1971. He received the B.S. and Ph.D. degrees in electrical engineering from National Taiwan University, Taipei, in 1993 and 1998, respectively.

His research interests include fiber laser mode locking, fabrication of fiber gratings and their applications, ultrashort pulse lasers, and solid-state lasers.

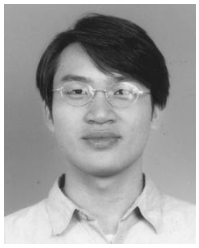

Gang-Chih Lin was born in Taoyuan, Taiwan, in 1974. He received the B.S. degree in electrical engineering and the M.S. degree in electrooptical engineering from National Taiwan University, Taipei, in 1996 and 1998, respectively. His thesis focused on the fabrication of fiber gratings with the interference technique of a 266-nm ultraviolet laser and the improvement of the sensitivity of temperature sensors based on fiber gratings.

C. C. Yang was born in Cha-I, Taiwan, in 1954. He received the B.S. degree in electrical engineering from National Taiwan University, Taipei, in 1976 and the M.S. and Ph.D. degrees in electrical engineering from the University of Illinois, Urbana-Champaign, in 1981 and 1984, respectively.

He then joined the Department of Electrical and Computer Engineering, The Pennsylvania State University, State College, as an Assistant Professor in 1984. He received his tenure and was promoted to Associate Professor in 1990. In 1993, he joined the Graduate Institute of Electro-Optical Engineering and the Department of Electrical Engineering, National Taiwan University, as a Professor. He has published more than 150 papers in technical journals and conferences. His research interests include ultrafast fiber and semiconductor optics, fabrication of fiber gratings and their applications, quantum-well intermixing and its applications, nonlinear optics, GaN-related materials and devices, and medical optics.